The Amblyopic Deficit and Its Relationship to Geniculo-Cortical Processing Streams

Robert F. Hess, Benjamin Thompson, Glen A. Gole and Kathy T. Mullen

J Neurophysiol 104:475-483, 2010. First published 12 May 2010;
doi: 10.1152/jn.01060.2009

Journal of Neurophysiology publishes original articles on the function of the nervous system. It is published 12 times a year (monthly) by the American Physiological Society, 9650 Rockville Pike, Bethesda MD 20814-3991.
 ISSN: 0022-3077, ESSN: 1522-1598. Visit our website at http://www.the-aps.org/.

J Neurophysiol 104: 475–483, 2010.
First published May 12, 2010; doi:10.1152/jn.01060.2009.

The Amblyopic Deficit and Its Relationship to Geniculo-Cortical Processing Streams

Robert F. Hess,[1] Benjamin Thompson,[1,2] Glen A. Gole,[3] and Kathy T. Mullen[1]

[1]*McGill Vision Research, Department of Ophthalmology, McGill University, Montreal, Canada;* [2]*Department of Optometry and Vision Science, University of Auckland, Auckland, New Zealand; and* [3]*Discipline of Paediatrics, University of Queensland, Royal Childrens Hospital, Brisbane, Australia*

Submitted 7 December 2009; accepted in final form 12 May 2010

Hess RF, Thompson B, Gole GA, Mullen KT. The Amblyopic deficit and Its relationship to geniculo-cortical processing streams. *J Neurophysiol* 104: 475–483, 2010. First published May 12, 2010; doi:10.1152/jn.01060.2009. Amblyopia or lazy eye is the most common cause of uniocular blindness in adults and is caused by a disruption to normal visual development as a consequence of unmatched inputs from the two eyes in early life, arising from a turned eye (strabismus), unequal refractive error (anisometropia), or form deprivation (e.g., cataract). Using high-field functional magnetic resonance imaging in a group of human adults with amblyopia, we previously demonstrated that reduced responses are observable at a thalamic level, that of the lateral geniculate nucleus (LGN). Here we investigate the selectivity of this deficit by using chromatic and achromatic stimuli that are designed to bias stimulation to one or other of the three ascending pathways (the parvocellular, magnocellular, and koniocellular). We find the greatest LGN deficit is for stimuli modulated along the chromatic, L/M cone opponent axis of color space, suggesting a selective loss of parvocellular function in the LGN. We also demonstrate a cortical deficit that involves all the visual areas studied (V1, V2, V3, VP, V3A, V4), and we find this is greatest for the two chromatic responses (S cone opponent and L/M cone opponent) versus the achromatic response, as might be expected from a loss of segregation of chromatic pathways in the cortex.

INTRODUCTION

Amblyopia (incidence 3%) is a disorder affecting visual development in humans that results in a uniocular visual loss in which individuals have impaired visual performance using one eye (the "amblyopic eye") and a normal "fixing" eye. Although, in human amblyopia, it has been known for some time that the visual deficit originates postretinally (Hess and Baker 1984; Hess et al. 1985), it has only recently been shown using functional magnetic resonance imaging (MRI) that the lateral geniculate nucleus (LGN) has reduced responses when driven by the amblyopic eye, indicating a functional deficit at the thalamic level (Hess et al. 2009b). This result in human vision is striking because the physiological origin of the deficit in animal models has been extensively investigated using single cell neurophysiology, and the current consensus is that the neural responses of both the retina (Cleland et al. 1980, 1982) and LGN are normal (Blakemore and Vital-Durand 1986; Derrington and Hawken 1981; Levitt et al. 2001; Sasaki et al. 1998; but see Chino et al. 1994; Ikeda and Tremain 1978; Sherman et al. 1975; Yin et al. 1997) even though the LGN layers that receive input from the affected eye exhibit histological abnormalities (Einon et al. 1978; Guillery 1972; Tremain and Ikeda 1982; von Noorden and Crawford 1992). Anomalous single cell responses are first found in layer 4c of striate cortex (cytoarchitectonic area 17 in cat and area V1 in primate).

Previously we revealed a functional LGN deficit in human vision that is common to all types of amblyopia by using a flickering checkerboard stimulus with combined modulation of luminance and color contrast (Hess et al. 2009b). The spatiotemporal broadband stimulus used was chosen to maximize the overall activity of the LGN and allow comparisons of monocular activation between eyes, but its disadvantage is that it cannot be used to assess the selectivity of the deficit for the different processing streams that relay information through the LGN. The LGN receives input from at least three distinct retinal pathways: the parvocellular pathway originating from the midget retinal bipolar cells (Derrington and Lennie 1984; Lee et al. 1990; Merigan et al. 1991), the magnocellular pathway emanating from the parasol retinal ganglion cells (Derrington and Lennie 1984; Kaplan and Shapley 1982; Lee et al. 1990; Solomon et al. 1999), and the koniocellular pathway receiving from specialized ganglion cells driven by short wavelength (S cone) photoreceptors (Chatterjee and Callaway 2003; Dacey and Packer 2003; Martin et al. 1997). All three cellular populations in the LGN are potentially activated by the checkerboard stimulus described above. In this study, we use spatiotemporal narrowband stimuli the contrast of which is modulated along different cardinal axes in color space to bias activation to each of these three LGN processing streams. For normal human vision, a previous study of the LGN has compared responses obtained to all three types of cardinal stimuli at equivalent cone contrasts and demonstrated that robust blood-oxygen-level-dependent (BOLD) responses to achromatic (Ach), L/M, and S cone opponent modulation can be obtained (Mullen et al. 2008). In the cortex, strong BOLD responses for chromatic stimuli modulated along both cardinal axes (activating L/M opponent and S cone opponent pathways) can be seen that involve all areas in the ventral pathway, with chromatic preferences revealed in areas V1 and VO (Brewer et al. 2005; Engel et al. 1997; Hadjikhani et al. 1998; Liu and Wandell 2005; McKeefry and Zeki 1997; Mullen et al. 2007, 2008; Wade et al. 2002; Wandell et al. 2005).

In this paper, we make simultaneous fMRI recordings from the LGN and cortex in a group of amblyopic subjects to investigate any selectivity of the LGN and cortical anomalies. Our results suggest that the LGN anomaly in amblyopia is greatest for L/M cone opponent stimuli, indicating that it is

Address for reprint requests and other correspondence: R. F. Hess, McGill Vision Research (H4.14), Dept. of Ophthalmology, 687 Pine Ave. W., Montreal, Quebec H3A 1A1, Canada (E-mail: robert.hess@mcgill.ca).

selective for parvocellular function. We also find a substantial cortical deficit affecting both striate and extra-striate areas, and we show that this is greater for chromatic as opposed to achromatic stimuli in the ventral pathway. These effects are consistent with a selective parvocellular deficit at the level of the LGN, where parvo-, magno-, and koniocellular pathways are segregated but that translates into a more general deficit for chromatic stimuli as a consequence of the mixing of the information from the two afferent chromatic pathways at the cortical level.

METHODS

Subjects and stimuli

We studied seven amblyopes selected to cover a range of etiologies including three strabismic, one mixed anisometropic-strabismic, one anisometropic, and two form-deprivation amblyopes, as detailed in Table 1. We measured the region of the retina used for fixation in all subjects using visuoscopy (Table 1), and we monitored the fixation eye-movements of all amblyopic subjects while they were viewing the stimulus in a control experiment run outside of the scanner using an in-house video monitoring of the pupil with subsequent off-line analysis of the variability of fixation. All subjects fixated on the central fixation mark provided, although the amblyopic eye was less steady than the fellow fixing eye (Table 1). The degree of unsteadiness was small, however, compared with the field size used (12°). All experiments were undertaken with the understanding and written consent of each subject. The study conforms to The Code of Ethics of the World Medical Association (Declaration of Helsinki), printed in the *British Medical Journal* in 1964.

Two different types of stimuli were used: a spatiotemporal broadband checkerboard stimulus with chromatic and achromatic contrast modulation (check size = 0.5°, square wave modulation = 16 Hz, contrast of 80%, field size of 10° height × 12° width) as illustrated in Fig. 1*A* or a narrowband ring stimulus sinusoidal in space and time (spatial frequency = 0.5 c/d, temporal frequency = 2 Hz), presented in a Gaussian temporal envelope (sigma = 125 ms). For the latter stimulus, as illustrated in Fig. 1*B*, there were three different types (RG, BY, and Ach) that isolated L/M cone opponent, the S cone opponent or the achromatic (luminance) postreceptoral mechanisms respectively (Mullen et al. 2007). The cone contrasts were set to high suprathreshold levels of 11% (Ach), 4% (RG), and 30% (BY). The circular stimulus was viewed as 16° (full width) by ~12° (full height), since stimulus height was limited top and bottom by the subject's placement in the bore of the magnet.

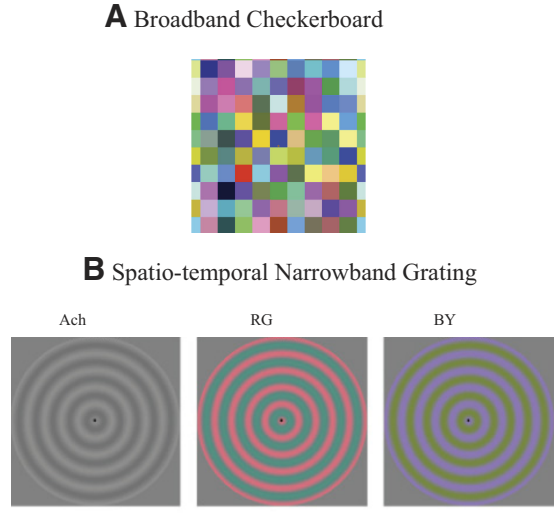

FIG. 1. Example of the 2 types of stimuli used. *A*: a broadband multicoloured checkerboard presented abruptly in time flickering at 16 Hz. *B*: spatiotemporal narrowband radial gratings sinusoidally modulated in space (0.5 c/d) and time (2 Hz), calibrated to activate the achromatic (Ach), L/M cone opponent (RG), or S cone opponent (BY) processing streams, respectively.

Experimental protocols

For the broadband checkerboard stimulus, a standard block design was used, as previously described (Hess et al. 2009b), composed of alternate presentations of the stimulus and blank (zero luminance) intervals (18 s of stimulus presentation, 18 s of blank, 10 blocks per run, 2 scanning runs). The checkerboard was presented in a two alternate forced choice (2AFC) paradigm within a 3 s cycle; each stimulus presentation was for 800 ms with an interstimulus interval of 200 ms and 1.2 s for response. Sinusoidal ring stimuli were presented in a 2AFC paradigm within a 3 s cycle; each stimulus was within a 500 ms time window in a temporal Gaussian contrast envelope (sigma = 125 ms) with an interstimulus interval of 500 ms and 1.5 s for the response, repeated six times for each condition (18 s). A roving baseline design was used whereby each block consisted of four conditions, the three types of ring stimuli (Ach, RG, BY) and a blank (mean luminance) interval with a fixation dot, as previously described (Mullen et al. 2007). The presentation order of these four conditions was pseudorandomized from block to block with each block presented 10 times in each of two scanning runs.

TABLE 1 *Clinical details for the seven amblyopic participants*

Subject and (Type of Amblyopia)	Refraction	Acuity	Eye Alignment	Fixation Centration	Fixation Variance,	History
JLK (Strabismic)	+0.75D +0.765D	6/5 6/48	3° LET	2° Eccentric	±0.74° ±2.7°	Large LET patching age 2yrs, surgery age 5 yrs.
BB (Strabismic)	+0.50/−0.50 × 160 +1.00/−0.25 × 180	6/5 6/600	5° LET	Central	±0.39° ±0.52°	Surgery to correct large angle eso age 7
CRF (Strabismic)	−2.75D −3.00D	6/6 6/240	3° LXT, 10 pd hypoT	4° Eccentric	±0.10° ±0.39°	L ET and surgery in infancy and age 25 yr
DLG (Aniso/strab)	−2.00/−2.75 × 15 −15.00/−2.25 × 180	6/7.5 CF	6° LXT	1° Eccentric	±0.15° ±0.36°	Anisometropia first detected in childhood, no surgery.
SJH (Anisomet.)	+7/−3.00 × 150 +2.50/−1.25 × 80	6/30 6/4.5	Ortho	Central	±0.38° ±0.35°	First Rx at age 19 yr
DJL (Deprivation)	+8.25/−1.00 × 90 +0.25D	CF 6/6	3° RET	6° Eccentric	±3.1° ±0.18°	2 ops for ET age 9
MLT (Deprivation)	−2.00D −1.50D	6/6 CF	19° XT	2° Eccentric	±0.42° ±1.8°	Cataract surgery age 7 yr

strab, strabismus; aniso, anisometrope; deprv, deprivation; R, right eye; L, left eye; ET, esotropia; XT, exotropia; HT, hypertropia; ortho, orthotropic alignment; D, dioptre sphere; FIX, monocular fixation; CF, count fingers.

To control for attentional modulation known to affect cortical and subcortical structures (O'Connor et al. 2002), subjects performed a 2AFC contrast discrimination task during all experiments that involved discriminating detectable differences in the contrast of pairs of stimuli within a stimulus cycle and responding with a button press (Hess et al. 2009b; Mullen et al. 2007). During the fixation (blank) epochs for the checkerboard stimuli, dummy button presses were made. For the ring stimuli during the fixation epoch, a similar contrast discrimination task was performed on a small white annulus surrounding the black fixation spot (Mullen et al. 2007). During scanning sessions feedback on the task was not given and percentages of correct data were not recorded. The contrast difference between stimulus pairs was large enough to be distinguishable by a normal eye (>90% correct on average). In a dummy scanning session, we measured the psychophysical performance using the checkerboard stimuli for the fixing and amblyopic eyes and responses were >90% correct for both fixing and amblyopic eyes (Hess et al. 2009b). For the ring stimuli, data collected on a group of normal subjects ($n = 5$) show that the contrast discrimination task was in the >90% correct range for Ach, RG, and BY stimuli with no significant difference between these three conditions. During all experimental paradigms participants viewed the central fixation mark monocularly and a tight-fitting eye patch was used to occlude the other eye. The same stimuli were presented to both amblyopic and fellow eyes and both the subject's eyes were tested in the same scanning session.

MRI

All MRIs were acquired using a 4T Bruker MedSpec system at the Centre for Magnetic Resonance, Brisbane, Australia. A transverse electromagnetic (TEM) head coil was used for radiofrequency transmission and reception (Vaughan et al. 2002). For the checkerboard stimulus, 256 T2*-weighted gradient-echo echoplanar images (EPI) depicting blood oxygen level dependent (BOLD) contrast (Ogawa et al. 1990) were acquired in each of 24 planes with TE 30 ms, flip angle = 90°, TR 1500 ms, in-plane resolution 3.1 x 3.1 mm and slice thickness 3 mm (0 mm gap). For the sinewave ring stimuli, 240 T2*-weighted gradient-echo echoplanar images (EPI) depicting blood-oxygen-level-dependent (BOLD) contrast were acquired in each of 36 planes with a TE of 30 ms, TR 3,000 ms, in-plane resolution 3.6 × 3.6 mm and a slice thickness of 3 mm (0.6 mm gap). These parameters were also used for the binocular LGN localization scans (see following text). All slices were taken parallel to the calcarine sulcus and arranged to include the anatomical location of the LGN. Two to three fMRI scans were performed in each session. Head movement was limited by foam padding within the head coil. In the same session, a high-resolution three-dimensional (3D) T1 image was acquired using an MP-RAGE sequence with TI 1,500 ms, TR 2,500 ms, TE 3.83 ms, and a resolution of 0.9 mm^3.

LGN localization

Left and right LGNs were localized in each participant using both anatomical and functional data. LGN localization data were acquired in a separate scanning session conducted under binocular viewing conditions. During scanning, participants viewed alternating blocks of the high contrast square wave checkerboard and the blank intervals with a small dim fixation dot, as described in the preceding text (see *Stimuli*) but with binocular rather than monocular viewing. Localization was based on the average of two scanning runs. Data were analyzed for each individual participant using a general linear model (GLM) analysis and statistical maps of *t*-values were visualized at the false discovery rate (FDR) corrected (Benjamini and Hochberg 1995) level of $q < 0.001$. LGNs were defined as a stimulus responsive region in the appropriate anatomical location (Kastner et al. 2004). Regions of interest (ROIs) were created by first identifying the peak voxel (i.e., the voxel the activity of which was most reliably correlated with the presentation of the stimulus) within the LGN region, then a cube of 1000 mm^3 (10 × 10 × 10 mm) was centered on the peak voxel and the ROI was defined as all voxels within the cube contiguous with the peak voxel, whose activity in response to the checkerboard stimulus was above threshold ($q < 0.001$). The Talairach coordinates of all the LGNs are given in Table 2.

Identification of cortical visual areas

Retinotopic mapping was performed using standard techniques (Dumoulin et al. 2003). Both polar angle and eccentricity maps were visualized on flattened representations of the cortical surface to allow the boundaries between visual areas to be defined. Only voxels within each cortical area that were activated significantly (FDR corrected $q < 0.001$) during binocular viewing of the LGN localization stimulus were included in the cortical ROIs to ensure that nonresponsive voxels were excluded.

Data analysis

Data analysis was conducted with the commercially available Brain Voyager analysis package version 1.9.10 (Brain Innovations, Maastricht, The Netherlands). Functional scans were high-pass filtered and motion corrected using subroutines within Brain Voyager. They were then aligned to each subject's high resolution anatomical images (resampled at 1 mm^3) and transformed to Talairach space (Talairach and Tournoux 1988). Time series data were extracted from the LGN region of interest for each individual participant using an event related averaging paradigm. For checkerboard stimuli, time series data were normalized to the preceding 2 TR (when the subject was viewing the blank) to provide a baseline for the %BOLD change measure. Average %BOLD change was calculated as the average %BOLD values within a temporal window starting 4 TR (6 s) after the onset of the stimulus and ending 4 TR after the offset of the stimulus. For the

TABLE 2 *LGN coordinates (mm) and volumes (mm^3) located in stereotaxic space for the seven subjects*

	Left				Right			
	Talairach Coordinates				Talairach Coordinates			
Participant	*x*	*y*	*z*	Vol, mm^3	*x*	*y*	*z*	Vol, mm^3
BB	−23	−26	−3	155	25	−25	2	86
CRF	−21	−27	−3	905	20	−27	−1	852
DJL	−19	−27	−3	91	18	−27	−1	147
JLK	−21	−24	−3	542	23	−22	−2	612
SJH	−23	−22	−4	243	25	−24	−2	283
MLT	−19	−28	1	518	20	−27	0	655
DLG	−19	−27	−3	91	18	−27	−2	147
Mean ± SD	−21 ± 2	−26 ± 2	−2 ± 2	409 ± 306	22 ± 3	−25 ± 2	−1 ± 1	439 ± 310

sinusoidal ring stimuli, %BOLD change for each stimulus type was calculated by normalizing to the last 4 TR of the fixation blocks. Average %BOLD change was then calculated using the same approach described in the preceding text with the exception that the averaging window was lagged by 1 TR (3 s) for this protocol as stimuli were not separated by a fixation interval.

For the checkerboard stimuli, %BOLD change data were analyzed using paired *t*-tests to compare activation generated by fellow eye stimulation with that generated by amblyopic eye stimulation for the LGN and each cortical area separately. For the sinewave ring stimuli, within subjects ANOVAs (df adjusted for sphericity using the Huynh-Feldt correction) with factors of eye (amblyopic vs. fellow) and chromaticity (Ach vs. RG vs. BY) were used to test for a differential pattern of responses between the activity generated by each eye for the different stimuli, as indicated by a significant interaction between eye and chromaticity. This analysis was performed separately for the LGN and V1. Data from extra-striate visual areas were analyzed together in the first instance using an ANOVA with factors of eye, chromaticity, and visual area (V2, V3, VP, V3A, and V4). As this analysis gave significant effects, separate ANOVAs were then conduced on each extra-striate area separately. ANOVAs were followed up by post hoc paired *t*-tests (2-tailed) that were conducted on the different chromaticity conditions within each eye separately to identify the differing patterns of responses. For ANOVAs in which a significant interaction was present a critical P value of $P < 0.05$ was employed for each post hoc paired *t*-test.

RESULTS

Comparison of responses in the LGN

Figure 2 shows the responses in the LGN for the amblyopic and fellow fixing eyes for a narrowband spatiotemporal stimulus modulated along the three different cardinal axes in color space (Fig. 2). Previously reported results in the LGN (Hess et al. 2009b their Fig. 2) for a broadband stimulus containing both luminance and chromatic contrast have shown a significantly stronger response to fellow fixing eye stimulation compared with amblyopic eye stimulation. For the spatiotemporal narrowband stimulus (Fig. 2), the LGN shows a differential pattern of response to the Ach, RG, and BY stimuli depending on whether the stimulus is presented to the fixing or amblyopic eye. The fellow fixing eye responds best to the RG stimulus, whereas the amblyopic eye does not. A within subjects ANOVA with factors of eye (fellow vs. amblyopic) and chromaticity (Ach vs. RG vs. BY) confirmed that this interaction between eye and chromaticity is significant [$F(2,12) = 5.05$, $P = 0.026$]. Post hoc paired *t*-tests revealed that this interaction is driven by a significantly higher response to the RG stimulus than to the Ach [$t(6) = 3.41$, $P = 0.014$] or the BY stimuli [$t(6) = 3.07$, $P = 0.022$] when the fixing eye was stimulated, with no such advantage occurring for the RG stimulus when the amblyopic eye was stimulated ($P > 0.05$). This suggests a selective loss of L/M cone opponent responses in the LGN when driven by the amblyopic eye.

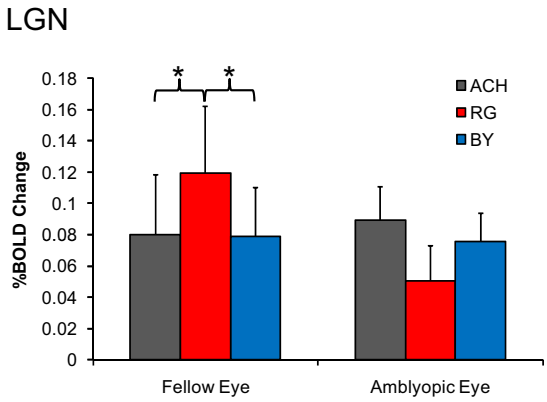

FIG. 2. Comparison of % blood-oxygen-level-dependent (BOLD) signals in the lateral geniculate nucleus (LGN) for fixing and amblyopic eyes for a spatiotemporal narrowband stimuli modulated along different axes in color space (Ach: gray bars; RG: red bars, BY: blue bars). Asterisks, statistical significance ($P < 0.05$). Error bars show average within subjects SE.

Comparison of responses in the cortex

We first show a voxel-based analysis of visual cortex conducted on the group data to illustrate the distribution of preferential activation between the fellow and amblyopic eyes for the chromatic versus the achromatic stimuli (Fig. 3). In this figure, we show the average group data for all seven subjects with separate representations for fellow eye stimulation (*top*) and amblyopic eye stimulation (*bottom*). Data are represented on computationally flattened representations of the left and right occipital lobes of one participant (*MLT*). The medial side of each panel represents the primary visual cortex that has been "cut" along the cortical representation of the horizontal meridian and the positions of the border locations based on *MLT*'s retinotopic map dividing the early visual areas V1, V2, V3, VP, V3A, and hV4 are marked by black lines. As these boundary positions are based on the retinotopic mapping data of one of our subjects, they are for illustration only.

This illustration is the result of a GLM analysis using a *z*-transformation based on the baseline components of the stimulus paradigm. Multiple comparisons were corrected using a false discovery rate of $q < 0.05$. The *t*-values represent the differences between the responses to the RG and Ach stimuli (Fig. 3*A*) or BY and Ach stimuli (Fig. 3*B*) with the red–yellow scale indicating a significantly greater response to the chromatic than achromatic stimuli and the blue–purple scale indicating a significantly greater response for achromatic than chromatic stimuli. The illustration shows quite strikingly in the fellow eye representation the presence of discrete visual cortical regions that respond preferentially to the isoluminant chromatic stimuli (RG or BY) over the achromatic stimuli (red-yellow scale), demonstrating the responses that are quite typical of a normal eye (Engel et al. 1997; Hadjikhani et al. 1998; Hess et al. 2009b; Liu and Wandell 2005; Mullen et al. 2007; Wade et al. 2002). In the amblyopic eye representations, however, these regions have almost completely disappeared and instead we see some preference for Ach over RG stimuli (blue-purple scale; Fig. 3*A*), or in the case of BY, mainly balanced responses for chromatic and achromatic stimuli (*B*). It is clear that the greater activation produced by the chromatic stimuli when the cortex was driven by the fixing eye (Fig. 3, *A* and *B, top*) is lost during amblyopic eye activation (Fig. 3, *A* and *B, bottom*) leaving a chromatic response that is now weaker than, or equal to, the achromatic one.

To provide an objective and quantitative analysis of the illustration depicted in Fig. 3 and to separate the responses according to the different stimulus types, chromatic and achromatic contrast, and visual area, we used a ROI analysis for the different cortical areas. Results for area V1 are shown in Fig. 4. The broadband checkerboard stimulus (Fig. 4*A*) pro-

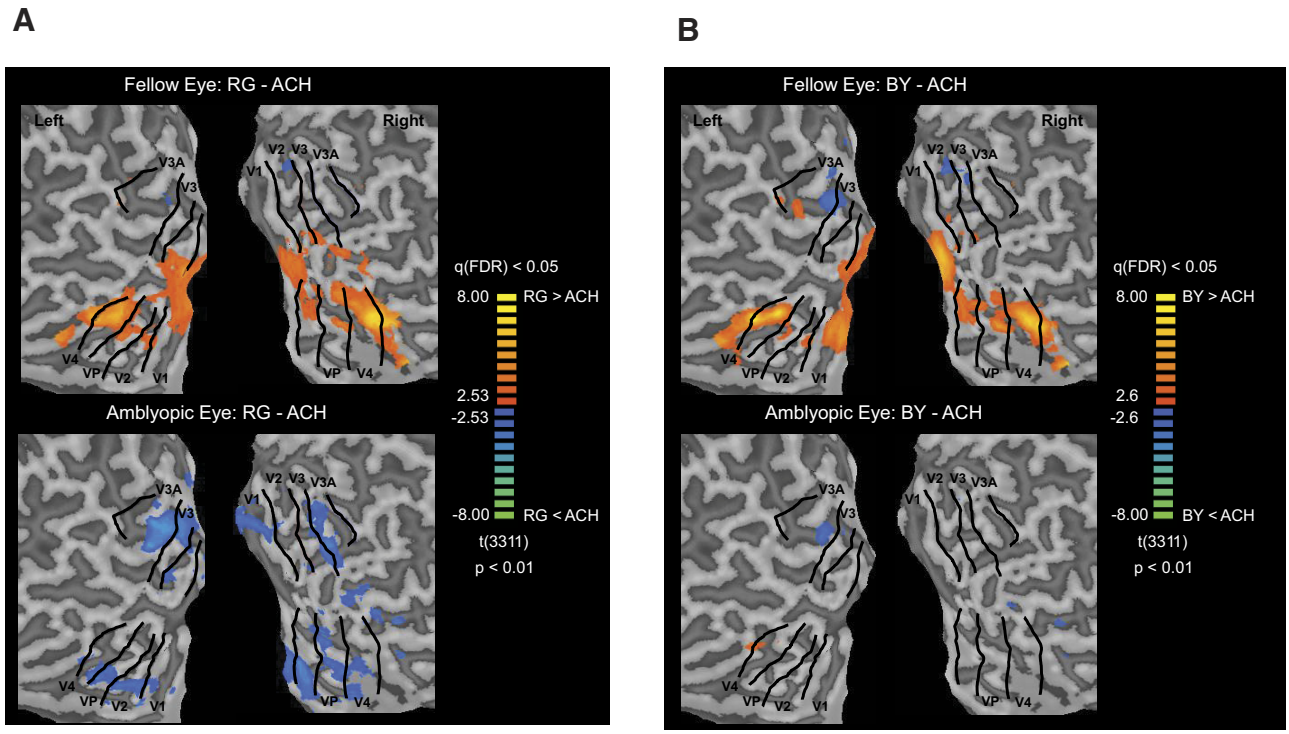

FIG. 3. The results of a group contrast between the RG-Ach conditions (*A*) and BY-Ach conditions (*B*) for the fellow fixing (*top*) and amblyopic eyes (*bottom*). Positive *t*-values (orange) represent a significantly greater activation of visual cortex by the chromatic than the achromatic stimuli, negative values (blue) represent the reverse. The flattened visual cortical surface of 1 participant (*MLT*) is used for the purposes of illustrating the group data. The medial edges of the flattened areas correspond to the representation of the horizontal meridian within the calcarine sulcus for this subject. The left hemisphere is shown on the reader's left and the right hemisphere on the right. The boundaries of the visual areas are based on MLT's retinotopic map and are presented only as a guide for interpretation of the group data.

duced a significantly weaker response to amblyopic eye stimulation than to fixing eye stimulation [$t(6) = 3.41$, $P = 0.014$]. For the narrowband ring stimulus (Fig. 4*B*), a significant difference between the relative responses to the Ach, RG, and BY stimuli was observed for the fixing versus amblyopic eyes in V1 [$F(2,12) = 11.07$, $P = 0.002$]. This interaction was driven by a significantly higher response to the two chromatic stimuli than to the Ach stimulus [Ach vs. RG, $t(6) = 4.94$, $P = 0.003$, Ach vs. BY, $t(6) = 3.40$, $P = 0.015$] when the fixing eye was stimulated with no such preference for chromatic stimuli when the amblyopic eye was stimulated. For the amblyopic eye, responses are similar across achromatic and chromatic conditions and hence these results demonstrate a selectively greater loss for chromatic stimuli.

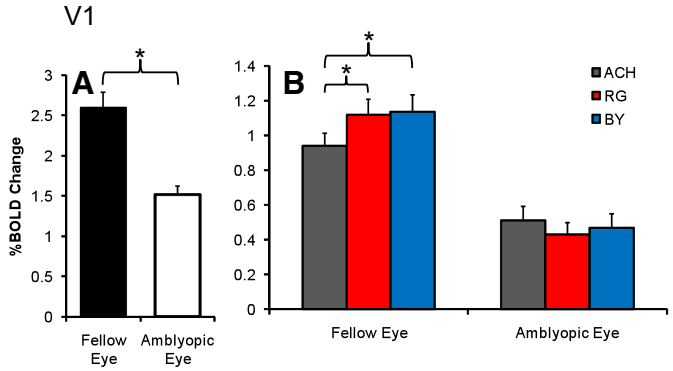

FIG. 4. Comparison of % BOLD signal in V1 for fixing and amblyopic eyes for broadband checkerboard stimuli (*A*) and spatiotemporal narrowband stimuli (*B*) modulated along different axes in color space (Ach: gray bars; RG: red bars, BY: blue bars). Asterisks, statistical significance ($P < 0.05$). Error bars show average within subjects SE.

Figure 5 shows a similar interocular comparison of fMRI responses for the broadband checkerboard (*left*) and spatiotemporal narrowband stimuli (*right*) for the extra-striate visual areas V2, V3, VP, V4, and V3A. Responses to the broadband checkerboard stimulus (Fig. 5, *left*) exhibited no interaction between eye and visual area [$F(4,24) = 1.64$, $P = 0.2$], indicating a consistent and significant deficit in the amblyopic eye response compared with that of the fixing eye across all extra-striate visual areas. Paired *t*-tests confirms that this difference between the fixing and fellow amblyopic eye is statistically reliable in all areas ($P < 0.05$) with the exception of V3A. For the spatiotemporal narrowband stimuli (Fig. 5, *right*), the results in extra-striate visual cortex show a change in the relative responses to the Ach, RG, and BY stimuli between the two eyes [$F(2,12) = 12.19$, $P = 0.001$, Fig. 5, *right*], similar to that found in the striate cortex. This difference in the pattern of activation between fixing and amblyopic eyes is due to a greater deficit for the two chromatic stimuli compared with the Ach stimulus for amblyopic eye activation. This characteristic chromatic loss occurs across all areas and does not depend on whether the fixing eye exhibits a significantly greater response to color (as in V2 and V4) or not (as in V3, VP, and V3A). The result is that the amblyopic eye is driven best by achromatic stimuli in all extra-striate areas except V4.

Figure 6 summarizes the different types of dependencies found for fixing and fellow amblyopic eyes for the spatiotemporal narrowband stimulus modulated along different axes in

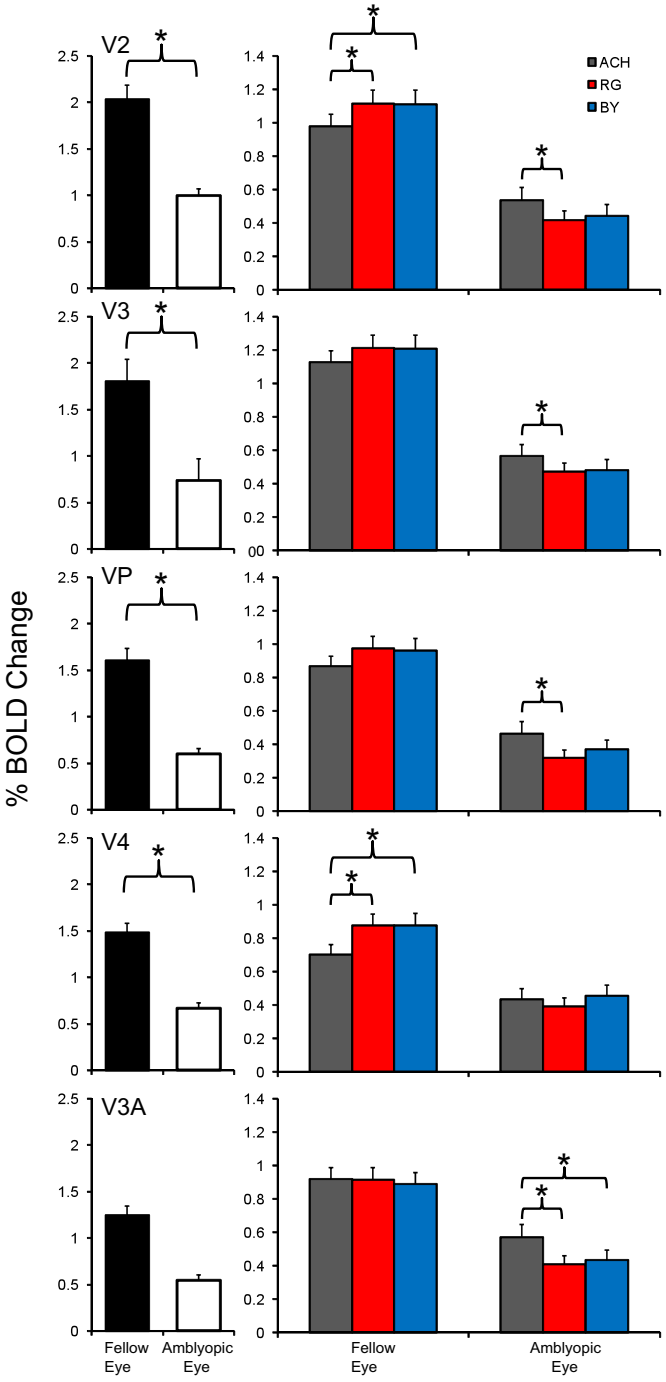

FIG. 5. Comparison of % BOLD signal in extra-striate visual areas (V2, V3, VP, V4, V3A) for fixing and amblyopic eyes for the broadband checkerboard stimuli (*left*) and spatiotemporal narrowband stimuli modulated along different axes in color space (Ach: gray bars; RG: red bars; BY: blue bars; *right*). The asterisks denote statistical significance ($P < 0.05$). Error bars show average within subjects SE.

color space. In the LGN, the best response for the fixing eye is to the L/M cone opponent modulation, whereas this produces the poorest response for the amblyopic eye. In striate and extra-striate cortex, the fixing eye stimulation produces the best response to chromatic stimuli whereas for the amblyopic eye the opposite is true; the best response is to the achromatic stimulus (Fig. 3). Thus in the cortex, the selective loss includes both types of chromatic response rather than just the L/M cone opponent response.

DISCUSSION

In a previous investigation, we showed, using a broadband checkerboard stimulus with combined luminance and color contrast, that there was reduced activation for amblyopic eye stimulation in the LGN (Hess et al. 2009b). Here we first demonstrate that this loss extends to both striate and extra-striate cortex. Second, we have investigated the selectivity of these losses by comparing fixing and amblyopic eye responses to spatiotemporal narrowband stimuli that were defined by luminance, L/M cone opponent, or S cone modulation. The thalamo-cortical pathway is composed of three separate projections, namely the magno-, parvo-, and koniocellular projections, each responding preferentially to achromatic (Derrington and Lennie 1984; Kaplan and Shapley 1982; Lee et al. 1990; Solomon et al. 1999), L/M cone opponent (Derrington and Lennie 1984; Lee et al. 1990; Merigan et al. 1991), or S cone isolating stimuli (Chatterjee and Callaway 2003; Dacey and

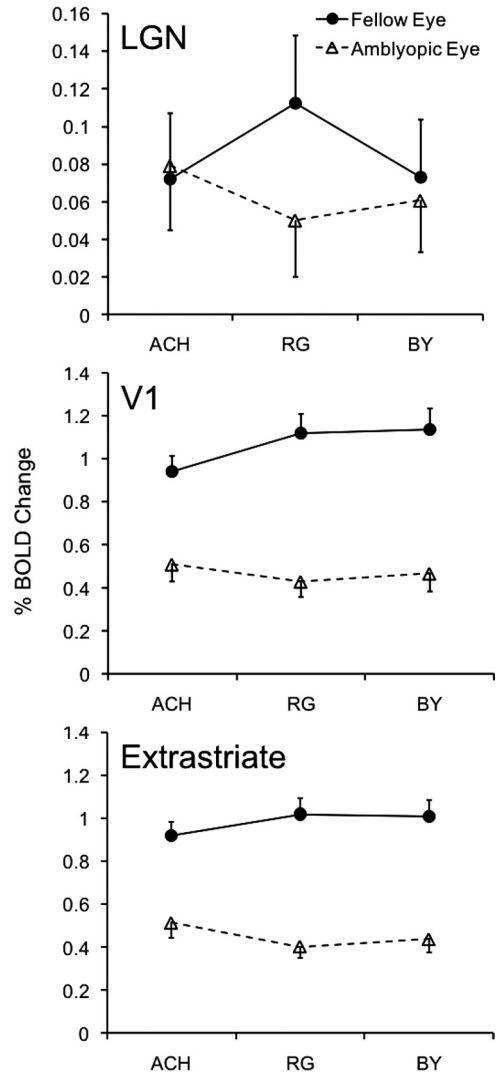

FIG. 6. Summary of the different dependencies for fixing and fellow amblyopic eye for the spatiotemporal narrowband stimulus in LGN and cortical visual areas as marked. The error bars are SE.

Packer 2003; Martin et al. 1997), respectively. Thus to assess whether the information carried by all three projections is affected equally in amblyopia or whether there is a selective deficit, we compared the fixing and amblyopic eye performance to each of these three diagnostic stimuli. Previous studies of normal subjects using fMRI have highlighted important features of the response to chromatic stimuli in both LGN and cortex. In the LGN, robust responses are found to red/green, achromatic, and blue/yellow stimuli at high contrasts (Mullen et al. 2008). In the cortex, there is also a robust response to color in V1 and in extra-striate areas of the ventral stream (Engel et al. 1997; Hadjikhani et al. 1998; Liu and Wandell 2005; McKeefry and Zeki 1997; Mullen et al. 2007; Wade et al. 2002). In addition, there is a relative boost of the response to S cone isolating stimuli in the cortex compared with the LGN (Mullen et al. 2008) consistent with the mixing of the parvo- and koniocellular geniculate inputs at the cortical level (Conway and Livingstone 2006; De Valois et al. 2000; Horwitz et al. 2007; Johnson et al. 2001, 2004; Lennie et al. 1990; Solomon and Lennie 2005; Wachtler et al. 2003). Robust responses to color, typical of the normal visual system, are also seen in the response of the fellow fixing eye of the amblyopes studied here (see Fig. 3). Our results indicate quite strikingly that the fMRI deficit exhibits a chromatic selectivity and that this varies from the thalamus to the visual cortex. In the LGN, there is a selective loss of function in the L/M cone opponent response shown by the fact that for the fixing eye, L/M cone opponent stimuli produce best activation, yet for the amblyopic eye, these stimuli produce the least activation. In the striate and extra-striate cortex, the activity driven by the amblyopic eye exhibits a selective chromatic deficit for both L/M cone opponent and S cone responses. At neither site do we find a significant correlation between the fMRI deficit and the visual acuity; more severe subjects did not necessarily exhibit larger losses.

These findings have a number of implications. First, they suggest that at the level of the LGN where the parvo-, magno-, and koniocellular pathways are physiologically separate (Derrington and Lennie 1984; Martin et al. 1997; Solomon et al. 1999) there may be a selective loss of parvocellular function because L/M cone opponent responses are mediated by parvocellular cells. Second, the fact that the deficit at the cortical level includes S cone as well as L/M cone opponent responses may be explained on the basis of the known mixing of parvo- and koniocellular cortical inputs. The population of cells in the LGN, as measured by single cell electrophysiology, exhibits a bimodal chromatic tuning reflecting the separate parvo-and koniocellular contributions, whereas in the cortex this becomes unimodal due to the presumed mixing of parvo- and koniocellular information (Conway and Livingstone 2006; De Valois et al. 2000; Horwitz et al. 2007; Johnson et al. 2001, 2004; Lennie et al. 1990; Solomon and Lennie 2005; Wachtler et al. 2003). Thus in terms of the current neurophysiology, the forms of both the lateral geniculate and cortical deficits are consistent with a primary loss of parvocellular geniculate function. Third, the fact that the LGN deficit is different from that found in striate cortex suggests a component of the LGN loss that cannot be solely due to feedback from striate cortex, implying a primary deficit in the LGN. This may be the result of less responsive cells or fewer cells (due to retrograde degeneration) responding to the input from the deprived eye.

Could the apparent loss of chromatic relative to achromatic sensitivity in the cortex driven by the amblyopic eye be a consequence of a loss affecting mainly central vision? The L/M cone opponent response is more confined to central vision, whereas the achromatic and S cone opponent response exhibit a more gradual fall-off with eccentricity measured both psychophysically (Mullen 1991; Mullen and Kingdom 2002; Mullen et al. 2005) and in terms of V1 BOLD activation (Mullen et al. 2007; Vanni et al. 2006). Hence a cortical deficit confined to central vision might produce a selective L/M cone opponent loss in an ROI analysis. Two findings argue against this. First, the selective chromatic cortical loss reported here occurs equally for L/M cone opponent and S-cone isolating stimuli, ruling out an explanation based solely on the regional nature of the deficit. Second, even though one previous study showed that the fMRI deficit in amblyopia is more centrally located (Li et al. 2007), this has not been a consistent finding (Conner et al. 2007).

The present study is the first to compare fMRI activation for stimuli whose contrast is defined by modulations in cardinal directions in color space designed to optimally activate magno-, parvo-, and koniocellular projections and find that the deficit at the level of the LGN is selective to parvocellular function while that at the cortex is selective for chromatic processing. We do not conclude however that the cortical deficit is limited to parvocellular function only. A number of studies have argued that parvocellular-driven cortical function is selectively compromised for the amblyopic eye input; for example, Miki et al. (2008) using fMRI argued for a selective loss for the parvocellular stimulus for one anisometropic amblyope. Mizoguchi et al. (2005), using PET, and Shan et al. (2000), using evoked potentials, came to a similar conclusion based on the response to different spatiotemporal stimulation. Hess et al. (2009a) reported a selective cortical fMRI deficit to high contrast stimuli when driven by the amblyopic eye and model this in terms of deficient parvocellular function at the level of the LGN. Although these studies use stimuli of different spatiotemporal or contrast composition in an effort to separate parvo-from magno-driven cortical function, this may not be ideal for two reasons; first there is evidence that parvo- and magnocellular geniculate input is mixed in cortical areas beyond 4C ± and — (Lachica et al. 1992; Levitt et al. 1994; Martin 1992; Merigan and Maunsell 1993; Nealey and Maunsell 1994; Sawatari and Callaway 1996; Sincich and Horton 2002; Vidyasagar et al. 2002) and second, suprathreshold stimuli of different spatiotemporal composition may not selectively activate each system (Merigan and Maunsell 1990; Merigan et al. 1991). Using a psychophysical approach, Grounds et al. (1983) report a selective loss in amblyopes of a spatiotemporal filter tuned to high spatial and low temporal frequencies claimed to reflect X-cell or parvocellular function. Davis et al. (2006) reported a color selective loss of psychophysical performance in the amblyopic eyes of late-onset strabismics as well as a chromatic selective visual evoked potential latency deficit (Davis et al. 2008) that they attribute to a selective loss of parvocellular function. One limitation of the study by Davis et al. (2006) was the use of a 3.2 c/d stimulus for the chromatic thresholds as this stimulus spatial frequency is likely to have significant luminance artifact (Faubert et al. 2000). A previous magnetoencephalographic study highlighted reduced power and longer latency in the cortical response to

L/M cone opponent stimuli of low-mid spatial frequency (1–2 c/d) for amblyopic eye stimulation (Anderson et al. 1999). Interestingly, this did not have a direct threshold psychophysical correlate, since thresholds for low-mid spatial frequency stimuli (0.5–2 c/d) were normal, being slightly reduced only at a higher spatial frequency (4c/d).

Strabismic and anisometropic amblyopia have been traditionally defined psychophysically in terms of deficient luminance contrast sensitivity (Gstalder and Green 1971; Hess and Howell 1977; Levi and Harwerth 1977), and little is known about the sensitivity to isoluminant chromatic stimuli in amblyopia. One study suggests that the threshold deficit is similar for chromatic and achromatic stimuli (Mullen et al. 1996), whereas another (Davis et al. 2006) suggests that the chromatic thresholds are more raised than achromatic thresholds. Amblyopic eyes also exhibit a greater positional deficit for chromatic stimuli (Mullen et al. 1996). The fact that there is little psychophysical loss of chromatic sensitivity may be because psychophysical thresholds are determined by relatively small numbers of neurons and may not reflect the type of suprathreshold processing by large neural populations that underlies fMRI measures. The present finding using fMRI, based on a mass neuronal response, may have an advantage in revealing suprathreshold effects. Future psychophysical research comparing suprathreshold rather than threshold chromatic and achromatic contrast processing may be successful in revealing a behavioral correlate of the BOLD color loss that we find in humans with amblyopia.

ACKNOWLEDGMENTS

We thank all of our subjects for giving up their time. We are particularly indebted to Dr. Joanne Wood of the Dept. of Optometry and Institute of Health and Biomedical Innovation, Queensland University of Technology, for the recruitment and scheduling of the patients at the onset of the study and for help in obtaining ethics approval and to A. Webber for patient recruitment.

GRANTS

This work was supported by a Canadian Institute of Health Research Grants MOP-53346 to R. F. Hess and MOP-10819 to K. T. Mullen and a Wesley Institute Research grant to G. A. Gole, R. F. Hess, and K. T. Mullen.

DISCLOSURES

No conflicts of interest, financial or otherwise, are declared by the author(s).

REFERENCES

Anderson SA, Holliday IE, Harding GF. Assessment of cortical dysfunction in human strabismic amblyopia using magnetoencephalography. *Vision Res* 39: 1723–1738, 1999.

Benjamini Y, Hochberg Y. Controlling the false discovery rate- a practical and powerful approach to multiple testing. *J R Stat Soc B Methodol* 57: 289–300, 1995.

Blakemore C, Vital-Durand F. Effects of visual deprivation on the development of the monkey's lateral geniculate nucleus. *J Physiol* 380: 493–511, 1986.

Brewer AA, Liu J, Wade AR, Wandell BA. Visual field maps and stimulus selectivity in human ventral occipital cortex. *Nat Neurosci* 8: 1102–1109, 2005.

Chatterjee S, Callaway EM. Parallel colour-opponent pathways to primary visual cortex. *Nature* 426: 668–671, 2003.

Chino YM, Cheng H, Smith EL 3rd, Garraghty PE, Roe AW, Sur M. Early discordant binocular vision disrupts signal transfer in the lateral geniculate nucleus. *Proc Natl Acad Sci USA* 91: 6938–6942, 1994.

Cleland BG, Crewther DP, Crewther SG, Mitchell DEM. Normality of spatial resolution of retinal ganglion cells in cats with strabismic amblyopia. *J Physiol* 326: 235–249, 1982.

Cleland BG, Mitchell DEM, Gillard-Crewther S, Crewther DP. Visual resolution of ganglion cells in monocularly deprived cats. *Brain Res* 192: 261–266, 1980.

Conner IP, Odom JV, Schwartz TL, Mendola JD. Monocular activation of V1 and V2 in amblyopic adults measured with functional magnetic resonance imaging. *J Aapos* 11: 341–350, 2007.

Conway BR, Livingstone MS. Spatial and temporal properties of cone signals in alert macaque primary visual cortex. *J Neurosci* 26: 10826–10846, 2006.

Dacey DM, Packer OS. Colour coding in the primate retina: diverse cell types and cone-specific circuitry. *Curr Opin Neurobiol* 13: 421–427, 2003.

Davis AR, Sloper JJ, Neveu MM, Hogg CR, Morgan MJ, Holder GE. Differential changes in color and motion-onset visual evoked potentials from both eyes in early- and late-onset strabismic amblyopia. *Invest Ophthalmol Vis Sci* 49: 4418–4426, 2008.

Davis AR, Sloper JJ, Neveu MM, Hogg CR, Morgan MJ, Holder GE. Differential changes of magnocellular and parvocellular visual function in early- and late-onset strabismic amblyopia. *Invest Ophthalmol Vis Sci* 47: 4836–4841, 2006.

De Valois RL, Cottaris NP, Elfar SD, Mahon LE, Wilson JA. Some transformations of color information from lateral geniculate nucleus to striate cortex. *Proc Natl Acad Sci USA* 97: 4997–5002, 2000.

Derrington A, Lennie P. Spatial and temporal contrast sensitivities of neurons in lateral geniculate nucleus of macaque. *J Physiol* 357: 219–240, 1984.

Derrington AM, Hawken MJ. Spatial and temporal properties of cat geniculate neurons after prolonged deprivation. *J Physiol* 314: 107–120, 1981.

Dumoulin SO, Hoge RD, Baker CL, Hess RF, Achtman RL, Evans AC. Automatic volumetric segmentation of human visual retinotopic cortex. *NeuroImage* 18: 576–587, 2003.

Einon G, Ikeda H, Tremain KE. Perikaryal size of cells in the lateral geniculate nucleus and amblyopia in cats reared with convergent squint (Proceedings). *J Physiol* 278: 50P, 1978.

Engel S, Zhang X, Wandell B. Colour tuning in human visual cortex measured with functional magnetic resonance imaging. *Nature* 388: 68–71, 1997.

Faubert J, Bilodeau L, Simonet P. Transverse chromatic aberration and color-defined motion. *Ophthalmic Physiol Opt* 20: 274–280, 2000.

Grounds AR, Holliday IE, Ruddock KH. Two spatio-temporal filters in human vision. II. Selective modification in amblyopia, albinism, and hemianopia. *Biol Cybern* 47: 191–201, 1983.

Gstalder RJ, Green DG. Laser interferometric acuity in amblyopia. *J Pediat Ophthalmol* 8: 251–256, 1971.

Guillery RW. Binocular competition in the control of geniculate cell growth. *J Comp Neurol* 144: 117–129, 1972.

Hadjikhani N, Liu AK, Dale AM, Cavanagh P, Tootell RB. Retinotopy and color sensitivity in human visual cortical area V8. *Nat Neurosci* 1: 235–241, 1998.

Hess RF, Baker CL. Assessment of retinal function in severely amblyopic individuals. *Vision Res* 24: 1367–1376, 1984.

Hess RF, Baker CL, Verhoeve JN, Tulunay Keesey U, France TD. The pattern evoked electroretinogram: its variability in normals and its relationship to amblyopia. *Invest Ophthal Visual Sci* 26: 1610–1623, 1985.

Hess RF, Howell ER. The threshold contrast sensitivity function in strabismic amblyopia: evidence for a two type classification. *Vision Res* 17: 1049–1055, 1977.

Hess RF, Li X, Lu G, Thompson B, Hansen BC. The contrast dependence of the cortical fMRI deficit in amblyopia; a selective loss at higher contrasts. *Hum Brain Mapp* In press.

Hess RF, Thompson B, Gole G, Mullen KT. Deficient responses from the lateral geniculate nucleus in humans with amblyopia. *Eur J Neurosci* 29: 1064–1070, 2009b.

Horwitz GD, Chichilnisky EJ, Albright TD. Cone inputs to simple and complex cells in V1 of awake macaque. *J Neurophysiol* 97: 3070–3081, 2007.

Ikeda H, Tremain KE. The development of spatial resolving power of LGN cells and its susceptibility to blur and strabismus. *Arch Ital Biol* 116: 375–384, 1978.

Johnson EN, Hawken MJ, Shapley R. The spatial transformation of color in the primary visual cortex of the macaque monkey. *Nat Neurosci* 4: 409–416, 2001.

Johnson EN, Hawken MJ, Shapley R. Cone inputs in macaque primary visual cortex. *J Neurophysiol* 91: 2501–2514, 2004.

Kaplan E, Shapley RM. X and Y cells in the lateral geniculate nucleus of macaque monkeys. *J Physiol* 330: 125–143, 1982.
Kastner S, O'Connor DH, Fukui MM, Fehd HM, Herwig U, Pinsk MA. Functional imaging of the human lateral geniculate nucleus and pulvinar. *J Neurophysiol* 91: 438–448, 2004.
Lachica EA, Beck PD, Casagrande VA. Parallel pathways in macaque monkey striate cortex: anatomically defined columns in layer III. *Proc Natl Acad Sci USA* 89: 3566–3570, 1992.
Lee BB, Pokorny J, Smith VC, Martin PR, Valberg A. Luminance and chromatic modulation sensitivity of macaque ganglion cells and human observers. *J Opt Soc Am A* 7: 2223–2236, 1990.
Lennie P, Krauskopf J, Sclar G. Chromatic mechanisms in striate cortex of macaque. *J Neurosci* 10: 649–669, 1990.
Levi M, Harwerth RS. Spatio-temporal interactions in anisometropic and strabismic amblyopia. *Invest Ophthalmol Vis Sci* 16: 90–95, 1977.
Levitt JB, Schumer RA, Sherman SM, Spear PD, Movshon JA. Visual response properties of neurons in the LGN of normally reared and visually deprived macaque monkeys. *J Neurophysiol* 85: 2111–2129, 2001.
Levitt JB, Yoshioka T, Lund JS. Evidence for interaction between diverent functional streams:Intrinsic cortical connections in macaque visual area V2. *J Comp Neurol* 342: 551–570, 1994.
Li X, Dumoulin SO, Mansouri B, Hess RF. Cortical deficits in human amblyopia: their regional distribution and their relationship to the contrast detection deficit. *Invest Ophthal Vis Sci* 48: 1575–1591, 2007.
Liu J, Wandell BA. Specializations for chromatic and temporal signals in human visual cortex. *J Neurosci* 25: 3459–3468, 2005.
Martin KAC. Parallel pathways converge. *Curr Biol* 2: 555–557, 1992.
Martin PR, White AJ, Goodchild AK, Wilder HD, Sefton AE. Evidence that blue-on cells are part of the third geniculocortical pathway in primates. *Eur J Neurosci* 9: 1536–1541, 1997.
McKeefry DJ, Zeki S. The position and topography of the human colour centre as revealed by functional magnetic resonance imaging. *Brain* 120: 2229–2242, 1997.
Merigan WH, Katz LM, Maunsell JH. The effects of parvocellular lateral geniculate lesions on the acuity and contrast sensitivity of macaque monkeys. *J Neurosci* 11: 994–1001, 1991.
Merigan WH, Maunsell JH. Macaque vision after magnocellular lateral geniculate lesions. *Vis Neurosci* 5: 347–352, 1990.
Merigan WH, Maunsell JH. How parallel are the primate visual pathways? *Annu Rev Neurosci* 16: 369–402, 1993.
Miki A, Siegfried J, Liu C-S, Modestino EJ, Liu G. Magno-and parvocellular visual cortex activation in anisometropia, as studied with functional magnetic resonance imaging. *Neuroophthalmology* 32: 187–193, 2008.
Mizoguchi S, Suzuki Y, Kiyosawa M, Mochizuki M, Ishii K. Differential activation of cerebral blood flow by stimulating amblyopic and fellow eye. *Graefe's Arch Clin Exp Ophthalmol* 243: 576–582, 2005.
Mullen KT. Color vision as a post-receptoral specialization of the central visual field. *Vision Res* 31: 119–130, 1991.
Mullen KT, Dumoulin SO, Hess RF. Color responses of the human lateral geniculate nucleus: selective amplification of S-cone signals between the lateral geniculate nucleno and primary visual cortex measured with high-field fMRI. *Eur J Neurosci* 28: 1911–1923, 2008.
Mullen KT, Dumoulin SO, McMahon KL, de Zubicaray GI, Hess RF. Selectivity of human retinotopic visual cortex to S-cone-opponent, L/M-cone-opponent and achromatic stimulation. *Eur J Neurosci* 25: 491–502, 2007.
Mullen KT, Kingdom FAA. Differential distribution of red-green and blue-yellow cone opponency across the visual field. *Visual Neurosci* 19: 109–118, 2002.
Mullen KT, Sakurai M, Chu W. Does L/M cone opponency disappear in human periphery? *Perception* 34: 951–959, 2005.
Mullen KT, Sankeralli MJ, Hess RF. Color and luminance vision in human amblyopia: shifts in isoluminance, contrast sensitivity losses, and positional deficits. *Vision Res* 36: 645–653, 1996.
Nealey TA, Maunsell JHR. Magnocellular and parvocellular contributions to the responses of neurons in macaque striate cortex. *Journal of Neuroscience* 14: 2069–2079, 1994.
O'Connor DH, Fukui MM, Pinsk MA, Kastner S. Attention modulates responses in the human lateral geniculate nucleus. *Nat Neurosci* 5: 1203–1209, 2002.
Ogawa S, Lee TM, Kay AR, Tank DW. Brain magnetic resonance imaging with contrast dependent on blood oxygenation. *Proc Natl Acad Sci USA* 87: 9868–9872, 1990.
Sasaki Y, Cheng H, Smith EL 3rd, Chino Y. Effects of early discordant binocular vision on the postnatal development of parvocellular neurons in the monkey lateral geniculate nucleus. *Exp Brain Res* 118: 341–351, 1998.
Sawatari A, Callaway EM. Convergence of magno- and parvocellular pathways in layer 4B of macaque primary visual cortex. *Nature* 380: 442–446, 1996.
Shan Y, Moster ML, Roemer RA, Siegfried JB. Abnormal function of the parvocellular visual system in anisometropic amblyopia. *J Pediatr Ophthalmol Strabismus* 37: 73–78, 2000.
Sherman SM, Wilson JR, Guillery RW. Evidence that binocular competition affects the postnatal development of Y-cells in the cat's lateral geniculate nucleus. *Brain Res* 100: 441–444, 1975.
Sincich LC, Horton JC. Divided by cytochrome oxidase: a map of the projections from V1 to V2 in macaques. *Science* 295: 1734–1737, 2002.
Solomon SG, Lennie P. Chromatic gain controls in visual cortical neurons. *J Neurosci* 25: 4779–4792, 2005.
Solomon SG, White AJ, Martin PR. Temporal contrast sensitivity in the lateral geniculate nucleus of a New World monkey, the marmoset *Callithrix jacchus. J Physiol* 517: 907–917, 1999.
Talairach J, Tournoux P. *Co-Planar Stereotaxic Atlas of the Human Brain.* New York: Thieme, 1988.
Tremain KE, Ikeda H. Relationship between amblyopia, LGN cell "shrinkage" and cortical ocular dominance in cats. *Exp Brain Res* 45: 243–252, 1982.
Vanni S, Henriksson L, Viikari M, James AC. Retinotopic distribution of chromatic responses in human primary visual cortex. *Eur J Neurosci* 24: 1821–1831, 2006.
Vaughan JT, Adriany G, Garwood M, Yacoub E, Duong T, DelaBarre L, Andersen P, Ugurbil K. Detunable transverse electromagnetic (TEM) volume coil for high-field NMR. *Magn Reson Med* 47: 990–1000, 2002.
Vidyasagar TR, Kulikowski JJ, Lipnicki DM, Dreher B. Convergence of parvocellular and magnocellular information channels in the primary visual cortex of the macaque. *Eur J Neurosci* 16: 945–956, 2002.
von Noorden GK, Crawford ML. The lateral geniculate nucleus in human strabismic amblyopia. *Invest Ophthal Vis Sci* 33: 2729–2732, 1992.
Wachtler T, Sejnowski TJ, Albright TD. Representation of color stimuli in awake macaque primary visual cortex. *Neuron* 37: 681–691, 2003.
Wade AR, Brewer AA, Rieger JW, Wandell BA. Functional measurements of human ventral occipital cortex: retinotopy and color. *Philos Trans R Soc Lond B Biol Sci* 357: 963–973, 2002.
Wandell BA, Brewer AA, Dougherty RF. Visual field map clusters in human cortex. *Philos Trans R Soc Lond B Biol Sci* 360: 693–707, 2005.
Yin ZQ, Crewther SG, Pirie B, Crewther DP. Cat-301 immunoreactivity in the lateral geniculate nucleus and visual cortex of the strabismic amblyopic cat. *Aust N Z J Ophthalmol 25 Suppl* 1: S107–109, 1997.